Trakya University Journal of Natural Sciences, 27(1), xx–xx, 2026
DOI: 10.23902/trkjnat.202573
www.tujns.org

Research Article

Chemical inhibition of the heat shock response downregulates *ERCC1* gene expression and shifts carboplatin-induced necrosis to apoptosis in TNBC cells

Beyza Reisoğlu[1], Mehmet Alper Arslan[2]*

[1]*Institute of Graduate Studies, Ondokuz Mayıs University, Department of Molecular Medicine, Samsun, Türkiye*
[2]*Ondokuz Mayıs University, Faculty of Medicine, Department of Medical Biology, Samsun, Türkiye*

Cite this article as: Reisoğlu, B., & Arslan, M. A. (2026). Chemical inhibition of the heat shock response downregulates *ERCC1* gene expression and shifts carboplatin-induced necrosis to apoptosis in TNBC cells. *Trakya University Journal of Natural Sciences, 27*(1), xx–xx.

Abstract

Background: Triple-negative breast cancer (TNBC) is an aggressive cancer type associated with poor prognosis and limited therapeutic options. Due to the absence of targetable receptors, conventional chemotherapy remains the primary treatment approach. ERCC1 is a critical component of the nucleotide excision repair system, responsible for repairing DNA damaged by platinum-based agents like carboplatin. Heat shock response (HSR) is a fundamental, stress-induced defense mechanism that supports cancer cell survival.

Aims: This study aims to investigate the effects of HSR inhibition by KNK437 on *ERCC1* gene expression and carboplatin sensitivity in the TNBC cell line MDA-MB-231.

Methods: The IC_{50} values of carboplatin and KNK437 were determined using WST-8 cytotoxicity assay. *ERCC1* gene expression levels were quantified by real-time quantitative polymerase chain reaction. Apoptotic and necrotic cell death induced by carboplatin and KNK437 was assessed by flow cytometry using FITC-Annexin V assay.

Results: The IC_{50} values of carboplatin and KNK437 were 247.5 μM and 89.74 μM, respectively. Carboplatin or KNK437 monotherapy significantly decreased *ERCC1* expression by 42.8% and 49.5%, respectively, while their combined application caused a 54.9% reduction. Furthermore, co-treatment markedly increased total cell death by 34.1% compared to carboplatin alone. Interestingly, necrosis induced by carboplatin shifted toward apoptosis upon co-treatment with KNK437, as confirmed by light microscopy and flow cytometry.

Özet

Dayanak: Üçlü negatif meme kanseri (TNBC), kötü prognoz ve sınırlı tedavi seçenekleri ile ilişkili agresif bir kanser türüdür. Hedeflenebilir reseptörlerin bulunmaması nedeniyle, geleneksel kemoterapi birincil tedavi yaklaşımı olmaya devam etmektedir. ERCC1, karboplatin gibi platin bazlı ajanlar tarafından hasar gören DNA'yı onarmaktan sorumlu olan nükleotid eksizyon onarım sisteminin kritik bir bileşenidir. Isı şoku yanıtı (HSR), kanser hücrelerinin hayatta kalmasını destekleyen, stres ile indüklenen temel bir savunma mekanizmasıdır.

Amaçlar: Bu çalışma, KNK437 aracılı HSR inhibisyonunun TNBC hücre hattı MDA-MB-231'de *ERCC1* gen ekspresyonu ve karboplatin duyarlılığı üzerindeki etkilerini araştırmayı amaçlamaktadır.

Yöntemler: Karboplatin ve KNK437'nin IC_{50} değerleri WST-8 sitotoksisite testiyle belirlenmiştir. *ERCC1* gen ekspresyon düzeyleri gerçek zamanlı kantitatif polimeraz zincir reaksiyonu ile ölçülmüştür. Karboplatin ve KNK437 tarafından indüklenen apoptotik ve nekrotik hücre ölümü, FITC-Annexin V testi kullanılarak akış sitometrisi ile saptanmıştır.

Bulgular: Karboplatin ve KNK437'nin IC_{50} değerleri sırasıyla 247,5 μM ve 89,74 μM olarak hesaplanmıştır. Karboplatin veya KNK437 monoterapisi *ERCC1* ekspresyonunu sırasıyla %42,8 ve %49,5 oranında azaltırken, bunların kombine uygulaması %54,9 oranında bir azalmaya neden olmuştur. Ayıca, kombine uygulama karboplatinin tek başına kullanımına kıyasla toplam hücre ölümünü %34,1 oranında belirgin şekilde artırmıştır. İlginç olarak, karboplatin tarafından indüklenen nekroz, KNK437 ile kombine uygulamada apoptoza

Edited by: *Ayşegül Çerkezkayabekir*
***Corresponding Author:** Mehmet Alper Arslan, **E-mail:** alper.arslan@omu.edu.tr*
***ORCID iDs of the author(s):** BR. 0000-0003-1149-9022; MAA. 0000-0002-3113-7195*

Received: 18 August 2025, **Accepted:** 9 December 2025, **Epub:** 13 January 2026

Conclusion: HSR inhibition by KNK437 enhances carboplatin sensitivity in TNBC cells and downregulates *ERCC1* gene expression. Given the aggressive nature of TNBC and its limited treatment options, our results suggest that KNK437 may offer therapeutic advantages when combined with carboplatin, particularly in contexts where carboplatin-induced necrosis contributes to inflammation-related complications.

Sonuç: Bulgularımız, KNK437 aracılı HSR inhibisyonunun TNBC hücrelerinde karboplatin duyarlılığını artırdığını ve *ERCC1* gen ekspresyonunu aşağı regüle ettiğini göstermektedir. TNBC'nin agresif doğası ve sınırlı tedavi seçenekleri göz önüne alındığında, sonuçlarımız KNK437'nin karboplatin ile kombine edildiğinde, özellikle karboplatin kaynaklı nekrozun inflamasyonla ilişkili komplikasyonlara katkıda bulunduğu durumlarda, terapötik avantajlar sunabileceğini göstermektedir.

Keywords: KNK437, carboplatin, *ERCC1*, heat shock response, triple-negative breast cancer

Introduction

Triple-negative breast cancer (TNBC) is a distinct breast cancer subtype characterized by the lack of estrogen receptor, progesterone receptor, and human epidermal growth factor receptor 2 (HER2) proteins (Bou Zerdan et al., 2022). TNBC represents a heterogeneous group of clinically challenging tumors, distinguished by early recurrence, poor overall survival, and development of resistance to chemotherapy. Compared to other subtypes, the therapeutic options for TNBC are limited as it does not respond well to hormone-based therapies or HER2-targeting drugs. Additionally, only a small fraction of TNBC patients respond effectively to novel targeted treatment methods and immunotherapeutic approaches. Therefore, platinum-based chemotherapy, either individually or in combination with these novel agents, continues to serve as the mainstay of TNBC treatment (Lee, 2023). However, there is an urgent need to identify new prognostic and predictive biomarkers for TNBC that can help improve treatment outcomes and guide more effective and individualized therapeutic strategies.

Platinum-based agents are compounds that exert cell apoptosis or necrosis by inducing the formation of adducts and crosslinks within the DNA helix, ultimately disrupting replication and transcription (Brabec & Kasparkova, 2005; de Sousa, 2014). A meta-analysis incorporating 12 clinical studies covering 4,580 patients reported that platinum-based chemotherapy significantly improves pathological complete response rates and prognosis in TNBC patients, with greater efficacy compared to non-platinum regimens (Lin et al., 2022). Carboplatin is a second-generation platinum-based chemotherapeutic agent that exhibits a more favorable toxicity profile compared to its predecessor, cisplatin, with notably suppressed nephrotoxicity, neurotoxicity, and gastrointestinal side effects. Several meta-analyses have demonstrated that the inclusion of carboplatin in neoadjuvant/adjuvant chemotherapy markedly improved disease-free and overall survival in TNBC (Bian et al., 2021; Pathak et al., 2022).

The nucleotide excision repair (NER) pathway is a critical DNA repair mechanism that removes a wide range of helix-distorting lesions, such as intrastrand crosslinks and bulky adducts induced by ultraviolet (UV) radiation, chemical mutagens, and certain chemotherapeutic agents. Excision repair cross-complementation group 1 (ERCC1) is a key component protein of the NER pathway; it forms a heterodimeric complex with Xeroderma Pigmentosum group F (XPF), an endonuclease, which catalyzes an excision step close to the site of DNA damage, crucial for the restoration of genomic integrity (Marteijn et al., 2014). Therefore, ERCC1 expression levels may be useful in predicting the responses of TNBC patients to platinum-based chemotherapy, with high or low ERCC1 levels associated with a poor or favorable response, respectively (Hashmi et al., 2025; Ma & El Kashef, 2017; Sidoni et al., 2008).

Heat shock response (HSR) is a highly conserved cell defense mechanism induced by various forms of stress, functioning to maintain protein homeostasis (proteostasis) under unfavorable conditions. Heat shock factor1 (HSF1) is the principal transcriptional regulator of the HSR and the expression of heat shock proteins (HSPs)/chaperones. Beyond its classical role in proteostasis, HSF1 promotes oncogenic transformation by coordinating a broad transcriptional network that encompasses pathways involved in protein synthesis, cell proliferation, survival, adhesion, and energy metabolism (Dai et al., 2007; Mendillo et al., 2012; Yun et al., 2019). KNK437 is a synthetic benzylidene lactam that inhibits the HSR by suppressing HSF1 transcriptional activity, and thus the expression of various HSPs, thereby exerting antitumor effects against various cancer types (Powers & Workman, 2007; Yun et al., 2019).

A recent study investigating the stability dynamics of the ERCC1–XPF complex proposed that the complex maintains its stability and cellular levels with the help of DCAF7, the proper folding of which is mediated by the molecular chaperone TRiC (Kawara et al., 2019). Based on this finding as well as evidence from previous research, we hypothesized that KNK437 may alter *ERCC1* expression in TNBC cells, thereby modulating the cytotoxicity induced by carboplatin. Therefore, the present study aims to elucidate the impacts of the HSR inhibitor KNK437 on *ERCC1* gene expression and carboplatin sensitivity in TNBC cells.

Materials and Methods

Human TNBC Cancer Cell Culture

The human TNBC cell line MDA-MB-231, obtained from the American Type Culture Collection (VA, USA), was used as a study model. The cells were cultured in GlutaMAX™ Dulbecco's

Modified Eagle Medium (Thermo Fisher Scientific, MA, USA) supplemented with 10% fetal bovine serum, 100 U/mL penicillin, and 100 µg/mL streptomycin. Cells were cultured at 37 °C in a Heracell 240i™ incubator and humidified atmosphere containing 5% CO_2 (Thermo Fisher Scientific) and subcultured every 2–3 days upon reaching a confluency of approximately 85%–90%. For passaging, the cells were detached using 0.05% trypsin–EDTA at 37 °C. Viable cells were counted with a hemocytometer after Trypan blue staining and reseeded at appropriate densities into new plates. All cell culture reagents used were purchased from Gibco (Thermo Fisher Scientific).

Cytotoxicity Analysis and IC_{50} Determination

To determine the IC_{50} values of carboplatin (C2538; Sigma-Aldrich Chemicals, MO, USA) and KNK437 (HY-100110; MedChemExpress, NJ, USA), cells were seeded into 96-well plates at a density of 1×10^4 cells/well, 24 h before drug treatments. A wide range of concentrations, each at 2-fold serial dilution, was employed to accurately determine the IC_{50}. The cells were treated with carboplatin or KNK437 at final concentrations of 2000, 1000, 500, 250, 125, 62.5, 31.25, 15.62, 7.81 µM; and 500, 250, 125, 62.5, 31.25, 15.62, 7.81 µM, respectively, for 48 h. Then, cell viability was assessed using the WST-8 assay (Abcam, Cambridge, UK), according to the manufacturer's instructions. In brief, 10 µL of the WST-8 reagent was added to each well, and the plates were incubated at 37 °C for 2 h. The OD_{460} was then measured using a Syn4 spectrophotometer (Biotek Instruments, Inc., VT, USA), in duplicate. The mean absorbance values were corrected by subtracting the absorbance of blank wells containing only culture medium. Dose-response curves were generated by setting the viability of untreated control cells to 100%, and IC_{50} values were calculated using the software GraphPad Prism version 10.0 (https://www.graphpad.com/).

Total RNA Isolation

Cells were seeded into 6-well plates at a density of 2.5×10^5 cells/well. The next day, they were treated with various concentrations of dimethyl sulfoxide (DMSO) (vehicle control for KNK437), carboplatin, KNK437, or carboplatin + KNK437 for 48 h. Following treatments, the culture medium was removed, and the cells were gently washed with 1X PBS. Then, TRIzol reagent (Invitrogen, Thermo Fisher Scientific) was added, the lysates were collected into a microcentrifuge tube by scraping, and incubated at room temperature for 10 min to allow complete homogenization. Chloroform was added to the lysates at a ratio of 1:5 (v/v), followed by vigorous shaking and incubation at room temperature for 5 min. For phase separation, solutions were cold-centrifuged using a 3K30 refrigerated benchtop centrifuge (Sigma Aldrich) at 11,500×g for 15 min. The clear upper aqueous phase containing the total RNA was carefully transferred to a fresh tube. An equal volume of 70% RNase-free ethanol was added slowly and gently mixed by pipetting. The mixture was then loaded onto a silica-based spin column provided with the FavorPrep™ RNA isolation kit (Favorgen Biotech Corp., Ping Tung, Taiwan), and then the manufacturer's instructions were followed. Total RNA was finally eluted in 50 µL of RNase-free water and stored at -80 °C until further use. RNA concentration was measured, and purity was assessed with a Jenway Genova Nano spectrophotometer (Bibby Scientific**,** Staffordshire, UK).

cDNA Synthesis and Quantitative Real-Time Polymerase Chain Reaction (qPCR)

For cDNA synthesis, 500 ng of the total RNA from each sample was reverse transcribed in a 20 µL reaction volume containing random hexamer primers, oligo(dT), and MMLV reverse transcriptase, provided with the iScript™ cDNA synthesis kit (Bio-Rad Laboratories, CA, USA), following the manufacturer's protocol. The thermal cycle profile used was as follows: 5 min at 25 °C (primer annealing), 30 min at 46 °C (cDNA synthesis), and 1 min at 95 °C (enzyme inactivation); GeneAmp 9700 PCR System (Applied Biosystems, Thermo Fisher Scientific). Freshly prepared cDNA was processed immediately for qPCR. The qPCR reaction mix with a total volume of 20 µL contained 1 µL of cDNA and 250 nM each of the forward and reverse primers specific to *ERCC1* and the reference *GAPDH*. An SsoAdvanced™ Universal SYBR® Green Supermix kit (Bio-Rad) was used, and the protocol provided was applied. The primer sequences were designed in-house using the PrimerBLAST tool (https://www.ncbi.nlm.nih.gov/tools/primer-blast/), set up with the universal primer design criteria. The 5'–3' sequences of the forward (F) and reverse (R) primers were F, *GAPDH*: CCATCTTCCAGGAGCGAGATC; R, *GAPDH*: GGCAGAGATGATGACCCTTTTG; and F, *ERCC1*: TTTGGCGACGTAATTCCCGA; R, *ERCC1*: CCTGCTGGGGATCTTTCACA. The thermal cycle profile employed was 30 sec at 98 °C (initial denaturation), followed by 40 cycles each of 10 sec at 98 °C (denaturation) and 30 sec at 60 °C (annealing/extension), and a CFX Connect™ Real-Time PCR Detection System (Bio-Rad) was employed. Melting curves were analyzed at the end of each run to confirm amplicon specificity. All reactions were performed in duplicate. Relative fold changes in *ERCC1* expression levels between the different drug treatment groups were calculated based on mean C_t values and utilizing the $2^{-\Delta\Delta Ct}$ method, and analyzed with REST 2009 software (QIAGEN, Venlo, Netherlands).

Agarose Gel Electrophoresis

To verify the specificity and expected sizes of the qPCR amplicons (146 and 175 bp for *GAPDH* and *ERCC1*, respectively), agarose gel electrophoresis was performed. Briefly, 2% agarose (HS-8000, Prona, Biomax) gel was prepared in 1X TAE buffer and added with a SafeView™ Classic Nucleic Acid Gel stain (Applied Biological Materials, BC, Canada). After the qPCR run was completed, 10 µL of the amplicons from two randomly selected wells per target gene (*GAPDH* and *ERCC1*) was mixed with 2 µL of 6X DNA loading dye (TriTrack, Thermo Fisher Scientific), and loaded into the gel wells along with a DNA ladder (GeneRuler 50 bp, Thermo Fisher Scientific). Electrophoresis was carried out at 100 V for 45 min using a Sub-Cell GT Horizontal Electrophoresis System (Bio-Rad), and the gel was subsequently imaged under UV transillumination on a ChemiDoc Go Imaging System (Bio-Rad).

Apoptosis/Necrosis Analysis by Annexin V Assay

To examine the effects of KNK437 on carboplatin-induced cytotoxicity in MDA-MB-231 cells, apoptosis and necrosis were assessed using an FITC-Annexin V apoptosis detection kit (BD Biosciences, NJ, USA), following the manufacturer's instructions. Cells were seeded into 6-well plates at a density of 2.5×10^5 cells/well. The next day, cells were treated with various concentrations of DMSO (vehicle control for KNK437), carboplatin, or KNK437, or combinations of carboplatin and KNK437 for 48 h. Next, the culture medium of each well containing the floating, dead cells was taken into a fresh tube; later, the media were pooled along with the corresponding adherent cells collected by trypsinization. The cells were gently washed with cold 1X PBS, and approximately 1×10^5 cells were resuspended in 100 µL of 1X Annexin V binding buffer. For staining, 2.5 µL of FITC-Annexin V and 2.5 µL of 7-AAD were added to each sample, gently mixed, and incubated at room temperature for 20 min in the dark. Finally, 400 µL of 1X Annexin V binding buffer was added to each tube, and cells were immediately analyzed using a BD FACS Calibur™ flow cytometer (BD Biosciences). Fluorescence signals in the FL1 (530/30) channel for FITC-Annexin V and the FL3 (670 LP) channel for 7-AAD were detected. A total of 20,000 gated events were acquired per sample, and quadrant lines were set employing the appropriate single- and double-stained controls. Data were analyzed using the BD CellQuest Pro™ software (BD Biosciences), and the proportions of necrotic (7-AAD$^+$ only), late apoptotic/necrotic (7-AAD$^+$ and FITC-Annexin V$^+$), and total dead (the sum of these two populations) cells were determined (in %) based on quadrant statistics.

Statistical Analysis

Statistical analyses and IC_{50} value calculations were performed using GraphPad Prism software version 10.0 (GraphPad Inc., CA, USA). Data are presented as the mean ± standard deviation (SD). Statistical evaluation of the relative fold changes in gene expression was conducted using the REST 2009 software (Qiagen). Student's t-test was applied for pairwise comparisons in the Annexin cell death assay. The p-values were considered statistically significant at $*p < 0.05$, $**p < 0.01$, and $***p < 0.001$.

Results

Determination of IC_{50} Values for Carboplatin and KNK437 in MDA-MB-231 Cells

To determine the IC_{50} values of carboplatin and KNK437, MDA-MB-231 cells were seeded in 96-well plates and treated with 2-fold serially increasing concentrations of carboplatin (7.81 µM to 2 mM) or KNK437 (7.81 µM to 500 µM) for 48 h. Cell viability was measured by the WST-8 assay, and dose-response curves were generated utilizing GraphPad Prism. The IC_{50} values obtained were 247.5 µM for carboplatin (Figure 1A) and 89.74 µM for KNK437 (Figure 1B), comparable to those of previous reports (Barrio et al., 2013; Wang et al., 2010).

Effects of Carboplatin and KNK437 on *ERCC1* Gene Expression as Single or Combined Treatments

To investigate the effects of carboplatin and KNK437, administered either alone or in combination, on *ERCC1* expression in MDA-MB-231 cells, a series of real-time qPCR experiments was conducted. Before proceeding with the main investigations, the lengths of the qPCR amplicons were verified by agarose gel electrophoresis. As shown in Figure 2A, amplicon bands corresponding to the expected sizes of the target genes—146 bp for *GAPDH* and 175 bp for *ERCC1*—were detected. The sharpness and positions of the bands, without any non-specific products, confirmed both the accuracy and specificity of the primer pairs designed for the target genes.

To assess the effect of carboplatin on *ERCC1* gene expression, the IC_{50} of the compound was used as the median dose, based on which the treatment concentrations were determined in a series of 2-fold dilutions. Accordingly, cells were treated with increasing concentrations of carboplatin (dissolved in water) ranging from 62.5 µM to 1 mM for 48 h. qPCR analysis revealed that *ERCC1* expression decreased significantly by 30%–40% across the concentrations tested compared to the untreated control (Figure 2B). Notably, carboplatin did not exhibit any dose-dependent suppression, as expression was reduced to similar levels, regardless of concentration.

To evaluate the effects of KNK437 on *ERCC1* expression, the cells were treated with increasing concentrations of KNK437 (dissolved in DMSO) ranging from 31.25 µM to 500 µM for 48 h. This concentration range was estimated based on the relative fold difference between the IC_{50} values of carboplatin and KNK437. To determine whether DMSO influenced *ERCC1* expression, the cells were also treated with only 2.5% (v/v) DMSO, the same concentration to which the cells were exposed when treated with the highest dose of KNK437 at 500 µM. As shown in Figure 2C, qPCR analysis revealed that *ERCC1* expression was remarkably reduced by 40%—60% across all concentrations tested, compared to the untreated control. However, treatment with DMSO alone also suppressed *ERCC1* expression by 60%, a level that was similar to that observed with 500 µM KNK437, indicating that the downregulation observed at 500 µM may not be due to KNK437, but rather DMSO (Figure 2C). Therefore, we decided to perform an additional set of qPCR experiments using DMSO alone to determine a DMSO concentration that did not interfere significantly with *ERCC1* expression.

The cells were exposed for 48 h to DMSO alone at 0.078%, 0.156%, 0.312%, and 0.625% (v/v), corresponding to the DMSO contents of the 15.62 µM, 31.25 µM, 62.5 µM, and 125 µM KNK437 treatments, respectively. Compared to the untreated control, *ERCC1* expression levels did not show any statistically significant alterations at any concentration tested ($p > 0.05$) (Figure 2D). However, as a slight decline was observed at 0.625% DMSO, a onefold lower concentration–0.312%–was selected for the subsequent combination treatment experiments. A comparative

analysis of Figures 2C and 2D clearly indicated that 62.5 μM KNK437 reduced *ERCC1* expression by approximately 50%, an effect which was also independent of any interference by DMSO.

Considering the proportional difference between the IC_{50} values of the two agents, 125 μM carboplatin was used in combination with 62.5 μM KNK437. To assess the synergistic effect of carboplatin and KNK437 on *ERCC1* expression, the cells were treated with only 125 μM carboplatin, only 62.5 μM KNK437, or a combination of the two for 48 h. Compared to the untreated control, carboplatin or KNK437 alone suppressed gene expression by 42.8% and 49.5%, respectively, whereas their combined application induced a 54.9% reduction (Figure 2E). Such results with single-agent treatments were consistent with our findings obtained previously at the two respective doses (Figure 2B for 125 μM carboplatin and Figure 2C for 62.5 μM KNK437). When the reduction ratios with single and combined treatments were compared, it was observed that KNK437 exerted a more robust influence than carboplatin in suppressing *ERCC1* gene expression (Figure 2E, carboplatin alone vs. combination: 21%, KNK437 alone vs. combination: 10%).

Effects of Carboplatin and KNK437 on Cell Death in MDA-MB-231 Cells as Single or Combined Treatments

To investigate the cytotoxic effects of carboplatin and KNK437, administered either alone or in combination, on MDA-MB-231 cells, a series of flow cytometry-based Annexin V assays was conducted. Based on previous experience from our studies investigating the impacts of carboplatin on the same cell line, a 1 mM dose was selected, as it consistently induced total cell death at ~40%. It was regarded as the baseline appropriate for the drug combination experiments, considering the potential of the second drug to either enhance or suppress this cytotoxicity ratio. Based on the proportional differences between the IC_{50} values of the two agents, doses of 250 and 500 μM KNK437 were selected.

Cells were treated with 2.5% DMSO alone (v/v; corresponding to the DMSO content at 500 μM KNK437), 1 mM carboplatin, 250 μM or 500 μM KNK437, and varying combinations of both drugs, for 48 h. The cells were subsequently visualized under an inverted phase-contrast light microscope (Figure 3A). Compared to the untreated cells (control), DMSO-only-treated cells exhibited a phenotypic shift toward an elongated, spindle-like morphology. Similar morphological changes were observed in the cells treated with 250 and 500 μM KNK437, suggesting that these effects were largely induced by DMSO. In contrast, the cells treated with only 1 mM carboplatin displayed morphological features, such as membrane disruption, cell disintegration, and swelling, which are characteristic of necrosis (white arrows, Figure 3A). Remarkably, a combination of carboplatin and KNK437 dramatically shifted the morphology, to a one characterized by rounded cells with intact membranes and evident shrinkage, indicative of apoptosis (black arrows, Figure 3A). The cell morphologies observed were consistent with the criteria well-established in the literature for distinguishing apoptosis and necrosis (Balvan et al., 2015).

Following the morphological analyses, to evaluate the cytotoxic impacts of carboplatin and KNK437, FITC-Annexin V assays were performed, followed by flow cytometry. MDA-MB-231 cells were treated for 48 h with carboplatin and KNK437, either alone or in combination, at the concentrations mentioned before, and the proportions of necrotic (7-AAD$^+$ only), late apoptotic/necrotic (7-AAD$^+$ and FITC-Annexin V$^+$), and total number of dead cells were quantified (%) by applying quadrant statistics (Figures 3B and 3C). Thus, our results indicate that KNK437 alone did not induce any remarkable cytotoxicity. At a lower dose of 250 μM, the total cell death rate remained comparable to that of the untreated and DMSO controls (~10%), while the 500 μM dose induced only a modest enhancement of 21%. In contrast, 1 mM carboplatin alone resulted in a total cell death of 42% (Figure 3C), with a majority of the dead cells located within the necrotic (lower right) quadrant (Figure 3B), consistent with their morphology, typical of necrotic cells, previously observed under light microscopy (Figure 3A). Remarkably, co-treatment with 250 μM KNK437 did not induce any substantial change compared to carboplatin alone (both 42%–44%, Figure 3C). However, a distinct shift from necrosis to late apoptosis was observed, reflected by a redistribution of the cell population from the lower right to the upper right quadrants (Figure 3B). Such an effect was more pronounced with a combination of carboplatin with 500 μM KNK437, at which the total cell death enhanced to 56.3%, representing a significant increase of 34.1% compared to carboplatin alone (Figure 3C). Such a trend was

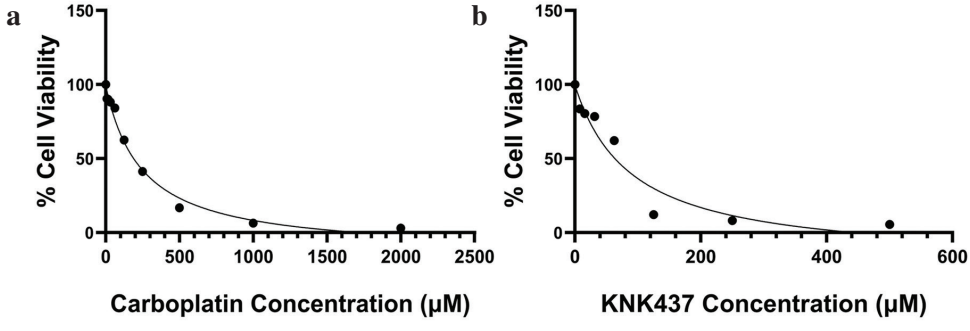

Figure 1. Dose-response curves and determination of IC_{50} values for carboplatin and KNK437 in MDA-MB-231 cells. Cells were seeded at a density of 10,000 cells/well in 96-well plates and treated for 48 h with 2-fold increasing concentrations of (a) carboplatin (7.81 μM–2 mM), or (b) KNK437 (7.81–500 μM). Cell viability was assessed using the WST-8 assay. Absorbance values for all drug concentrations were measured in duplicate. The dose-response curves were generated by considering the viability of the untreated control cells as 100%, and IC_{50} values were calculated using GraphPad Prism software.

again largely due to the shift from necrosis (carboplatin alone) to apoptosis (combination with KNK437) (Figure 3B), consistent with their respective morphologies previously observed using light microscopy (Figure 3A). Collectively, our light microscopy and flow cytometry findings demonstrate that necrosis induced by carboplatin is replaced by apoptosis upon co-treatment with KNK437.

Discussion

Platinum-based chemotherapy, either as a monotherapy or combined with other cancer therapeutics, remains the cornerstone of current TNBC treatments. However, a critical need to discover reliable prognostic and predictive biomarkers and thereby enhance clinical outcomes, guide personalized treatment approaches, and elucidate the mechanisms underlying therapeutic resistance and recurrence still arises (Lee, 2023). The present study investigated the effects of single and combined applications of carboplatin and the HSR inhibitor KNK437 on apoptosis or necrosis-induction and *ERCC1* gene expression in the TNBC cell line MDA-MB-231.

The NER pathway is a mechanism critical to the repair of DNA damage caused by platinum-based chemotherapeutic agents. Upregulation of the genes involved in the NER enables cancer cells to effectively repair such damage, ultimately contributing to the development of resistance (de Sousa, 2014).

Elevated *ERCC1* mRNA and protein levels in cisplatin-resistant human ovarian cancer cells have been reported (Li et al., 2000). Similarly, *ERCC1* mRNAs were markedly higher in tumor biopsies of cisplatin-resistant gastric cancer patients (Metzger et al., 1998). In contrast, *XPA*, *XPF*, and *ERCC1* expression was low in cisplatin-sensitive testicular cancer cell lines, indicating their limited capacity to mitigate cisplatin-induced DNA damage (Welsh et al., 2004). Similarly, in our study, since MDA-MB-231 cells are not resistant to carboplatin, their primal response to carboplatin-induced DNA damage was to suppress *ERCC1* expression (Figure 2B), and commit to cell death rather than to DNA repair and survive (Figure 3C). Moreover, a combination of carboplatin and KNK437 further decreased *ERCC1* expression (Figure 2E), thereby enhancing the sensitivity of MDA-MB-231 cells to carboplatin and ultimately increasing cell death levels compared to that induced by carboplatin alone (Figure 3C). This finding of ours where HSF1 was chemically inhibited by KNK437, is consistent with a previous report in which the shRNA-mediated knockdown of *HSF1* also rendered MDA-MB-231 cells more sensitive to carboplatin (Desai et al., 2013).

DMSO is a polar, amphipathic, aprotic organic molecule that is ideal for dissolving poorly soluble polar and non-polar compounds, due to which it is widely used in toxicology and pharmacology studies, and also for the cryopreservation of cells. Although conventionally DMSO is considered non-toxic at concentrations ≤ 10% (v/v),

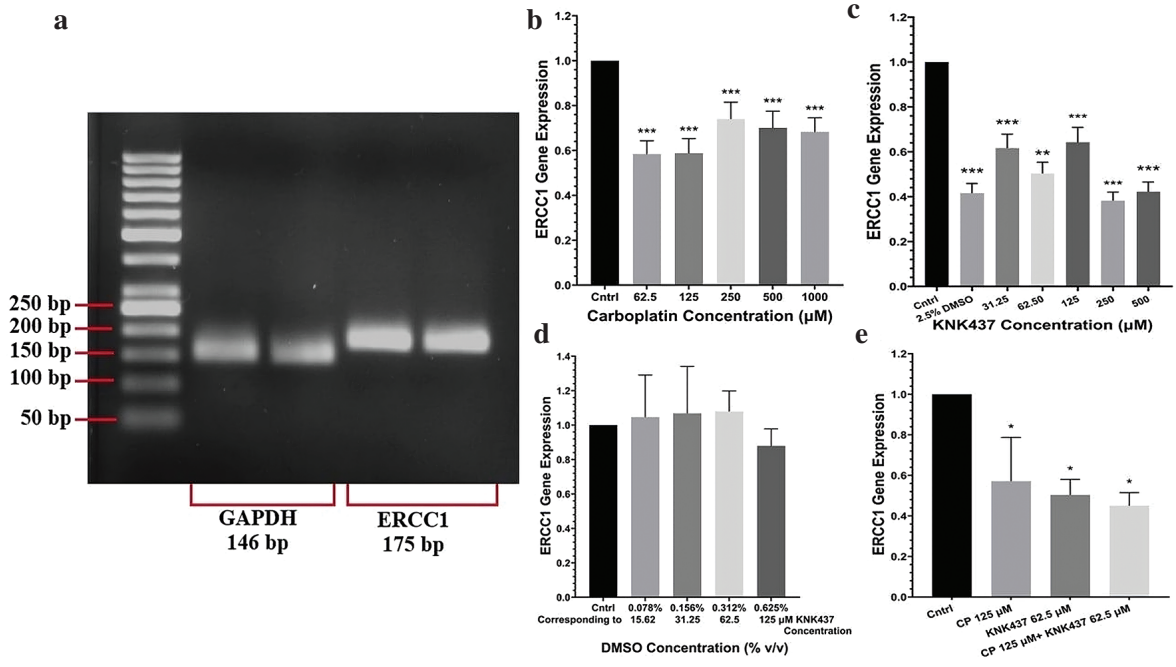

Figure 2. Carboplatin and KNK437 decreases *ERCC1* gene expression individually, with further suppression when used in combination. (a) Verification of the specificity of amplified qPCR products for *GAPDH* and *ERCC1* by agarose gel electrophoresis. Following qPCR, 10 µL of each amplicon was loaded onto a 2% agarose gel, electrophoresed, and visualized under UV light. Expected amplicon sizes were 146 bp for *GAPDH* and 175 bp for *ERCC1*. (b–d) The relative *ERCC1* expression levels in MDA-MB-231 cells treated for 48 h with increasing concentrations of carboplatin (b), KNK437 (c), or DMSO (d). (e) The relative *ERCC1* gene expression levels in cells treated for 48 h with carboplatin, KNK437, or their combination. For all experiments, 500 ng of total RNA isolated from each sample was converted to cDNA, and real-time qPCR was performed using 1 µL of the cDNA with gene-specific primers and SYBR Green master mix. Fold changes in gene expression and their statistical significance were analyzed using the REST 2009 software, and pairwise comparisons were made relative to the untreated control (*$p < 0.05$, **$p < 0.01$, ***$p < 0.001$).

exposure of 3D cardiac and hepatic microtissues to DMSO at levels as low as 0.1% (v/v) markedly altered the functioning of cellular processes, including significant changes in transcription and translation as well as the epigenetic landscape, as revealed by comprehensive transcriptomic, proteomic, and DNA methylation profiling (Verheijen et al., 2019). To further elucidate the cytotoxic effects of DMSO at the concentration ranges (0.1%–1.5% [v/v]) typically used in cell-based studies, epithelial colon cancer cells were treated with DMSO; and it has been reported that DMSO alters both DNA and protein topologies, in addition to significantly suppressing the expression of certain proteins at concentrations ≥ 0.5% (v/v) (Tuncer et al., 2018). Similarly, we observed that DMSO, used as a solvent for KNK437, reduced *ERCC1* expression at concentrations ≥ 0.625% (v/v) (Figures 2C and 2D). Therefore, additional qPCR assays using increasing concentrations of only DMSO were conducted to determine a concentration that did not impact *ERCC1* transcription. Consequently, we identified 0.312% (v/v) as the maximum level that did not induce any detectable background suppression of *ERCC1* expression, and thus, 62.5 µM was the highest KNK437 concentration that could be used free of any interference by DMSO (Figure 2D). The subsequent qPCR experiments involving combined drug treatments employed this level as the reference (Figure 2E).

The Annexin V cell death assays conducted later demonstrated that even 2.5% (v/v) DMSO, corresponding to 500 µM KNK437, did not remarkably enhance cell death compared to the untreated control (Figure 3C), but induced distinct changes in cell morphology, including elongation and the production of spindle-like extensions (Figure 3A). In line with the findings of the two studies mentioned earlier, our results highlight the need for considerable caution when using DMSO as a solvent, as its toxic effects can manifest at the level of gene expression without being reflected by cell death rate. Although DMSO is widely regarded as a "universal solvent" with a diverse range of biological applications, its potential adverse effects should not be overlooked, and the working concentration should be minimized to the extent possible.

The effects of DMSO on TNBC cell morphology observed in our study are consistent with several previous reports. For instance, polyclonal human ovarian cancer cells exposed to 1% DMSO for several days displayed a similar spindle-like morphology and a monolayer growth pattern characterized by contact inhibition (Grunt et al., 1991), as was also reported in several human lymphoblastoid and HeLa cell lines exposed to 2% DMSO suggesting that such a morphological response was independent of tissue origin (Aranda-Anzaldo et al., 2024). Our observations agreed with these studies, as exposure to 2.5% (v/v) DMSO caused the MDA-MB-231 cells to adopt a spindle-like morphology (Figure 3A). Similar morphological changes were also detected in cells treated with 250 and 500 µM KNK437 (Figure 3A), which were most likely due to the background effect of DMSO.

KNK437 inhibits the HSR by blocking the transcriptional activity of HSF1 (Powers & Workman, 2007). Our observation that

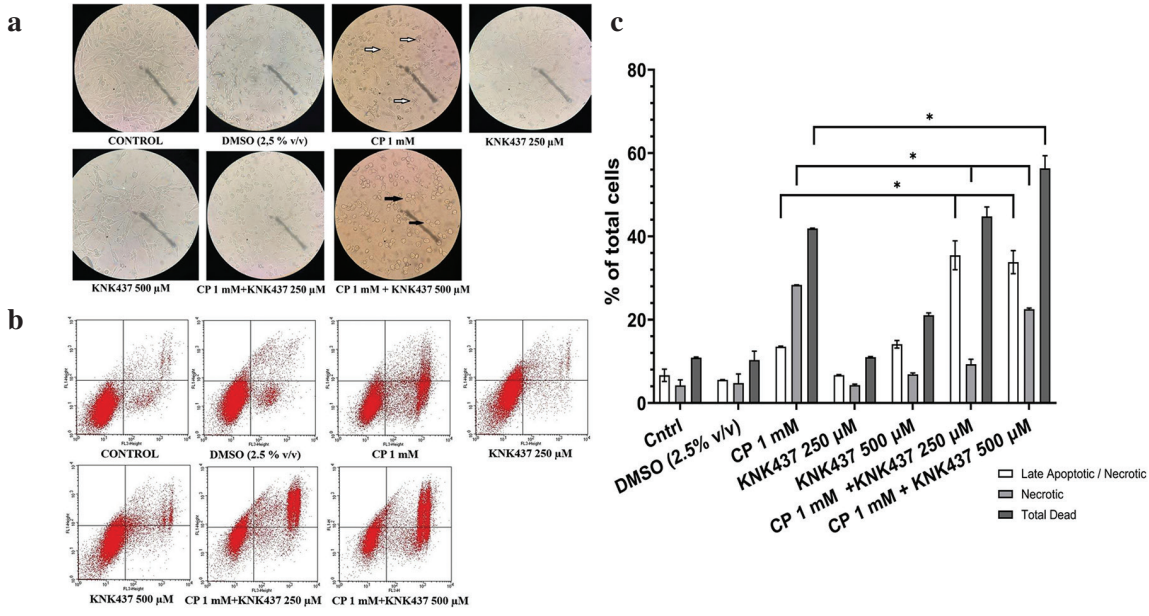

Figure 3. KNK437 co-treatment enhances the cytotoxic effects of carboplatin and shifts carboplatin-induced necrosis toward apoptosis. (a) Representative light microscopy images showing cell morphologies following 48 h of treatment with the indicated concentrations of DMSO, carboplatin, KNK437, or their combinations (100X magnification). White and black arrows indicate the necrotic and apoptotic cells, respectively. (b) Representative flow cytometry plots displaying the cell population distribution assessed by the FITC-Annexin V/7-AAD cell death assay. Following 48 h of treatment with the indicated agents at the concentrations specified, cells were collected by trypsinization, stained, and analyzed by flow cytometry using FL1 (y-axis) and FL3 (x-axis) channels to detect the FITC-Annexin V and 7-AAD-associated fluorescence signals, respectively. (c) Quantification of the proportions of cells in the upper right (late apoptotic/necrotic) and lower right (necrotic) quadrants from (b), and their sum (total dead). Data represent the mean ± SD of two independent experiments (*$p < 0.05$, Student's t-test, pairwise comparisons relative to 1 mM carboplatin alone).

ERCC1 gene expression decreased significantly even at low doses of KNK437 (31.25 μM, Figure 2C) suggested that *ERCC1* might indeed be a genuine transcriptional target of HSF1. To explore this possibility, we comprehensively reviewed the literature and examined the supplementary data of high-throughput genome-wide transcriptomic and chromatin immunoprecipitation microarray studies conducted on HSF1. In two such reports, *ERCC1* was listed among the genes that are transcriptionally upregulated by HSF1 (Kovács et al., 2019; Page et al., 2006). These microarray-based findings provide a possible explanation for the reduction in *ERCC1* expression induced by KNK437, and further support the notion that *ERCC1* might be a bona fide HSF1 target gene. Future studies employing chromatin immunoprecipitation to assess HSF1 binding at the *ERCC1* promoter, combined with functional luciferase reporter assays, are warranted to provide direct evidence of such transcriptional regulation.

Carboplatin acts by binding to DNA and inducing the formation of adducts and crosslinks, which disrupt replication and transcription, thereby activating signaling pathways that ultimately lead to apoptosis or necrosis (Brabec & Kasparkova, 2005; de Sousa, 2014). In our study, morphological aberrations such as membrane disruption, disintegration, and swelling observed in cells treated with 1 mM carboplatin were indicative of necrosis (white arrows, Figure 3A). This finding was also supported by our flow cytometry-based apoptosis/necrosis analysis, which revealed necrosis as the predominant mode of death in MDA-MB-231 cells exposed to only carboplatin (Figure 3B). In conjunction, these results indicate that carboplatin primarily induces necrosis rather than apoptosis in MDA-MB-231 cells. Such an association between carboplatin and necrosis is also supported by the literature, as evidenced by reports of a scleroderma patient with lung cancer who developed digital necrosis following chemotherapy (Clowse & Wigley, 2003) and of a lymphocytic leukemia patient who died due to acute liver necrosis following carboplatin therapy (Hruban et al., 1991).

When cells were treated with a combination of carboplatin and KNK437, marked changes in cell morphology were observed compared to those treated with only carboplatin, such as rounded, shrunken cells with a largely preserved membrane integrity, which are characteristic features of apoptosis (black arrows, Figure 3A). These results were supported by our further flow cytometry-based apoptosis/necrosis analysis, where a redistribution of the cell population from the lower right to the upper right quadrants indicated apoptosis as the predominant mode of cell death in response to combined carboplatin and KNK437 exposure (Figure 3B). Notably, the cell morphologies observed were fully consistent with the well-established characteristics for apoptosis and necrosis reported in the literature (Balvan et al., 2015). In summary, these results indicate that in MDA-MB-231 cells, necrosis induced by carboplatin alone is replaced by apoptosis when combined with KNK437. The pro-apoptotic influence of KNK437 is corroborated by a previous study where the inhibition of HSR by KNK437 significantly enhanced the apoptosis induced by the proteasome inhibitor bortezomib in multiple myeloma cells and mouse embryonic fibroblasts, as evidenced by increased Annexin V staining and DNA fragmentation (Voorhees et al., 2007). Altogether, our study demonstrates that KNK437 co-treatment promotes apoptosis at low (250 μM) and high (500 μM) doses, and enhances carboplatin-induced cytotoxicity by 34.1% at the higher dose (Figure 3C). These findings underline the promising potential of KNK437 to improve the efficacy of carboplatin chemotherapy against TNBC.

Study Limitations

There were several limitations to our study. First, the drug concentrations used to assess *ERCC1* gene expression could not be directly employed in the Annexin V cell death assays, as these doses were too low to produce any differential cytotoxic response in this assay. However, as the higher KNK437 doses (250 and 500 μM) applied could have interfered with *ERCC1* gene expression due to their high DMSO content, the effects observed in cell death might result from other biological actions of KNK437. Second, only a single TNBC cell line was used throughout the study, which may limit the generalizability of our findings to other TNBC models. Third, *ERCC1* expression was assessed only at the mRNA level; therefore, potential post-transcriptional regulations or functional effects at the protein level could not be evaluated. Future studies involving additional TNBC cell lines and functional analyses of ERCC1 protein would help provide a more comprehensive understanding of the underlying mechanisms.

Conclusion

In conclusion, our findings reveal that the chemical inhibition of the HSR by KNK437 downregulated *ERCC1* expression and increased carboplatin sensitivity in TNBC cells. Interestingly, necrosis triggered by carboplatin was replaced by apoptosis when it was administered in combination with KNK437. Excessive inflammation evoked by chemotherapy-induced necrosis at the tumor microenvironment is well known to contribute to adverse clinical outcomes such as therapy resistance, tumor progression, angiogenesis, and metastasis (Akkız et al., 2025; Vyas et al., 2014). In such cases, as suggested by the present study, redirecting tumor cells from necrosis to apoptosis and thereby evading inflammation through KNK437 co-administration may offer significant therapeutic advantages for the treatment of TNBC—an aspect that requires further investigation by more comprehensive studies in the future.

Acknowledgements

This study is based on the master's thesis of Beyza Reisoğlu, conducted under the supervision of Assist. Prof. Dr. M. Alper Arslan as the thesis advisor. We would like to thank OMU-KÖKMER Center for their assistance with flow cytometry used in Annexin V cell death assay.

Ethics

Ethics Committee Approval: Not applicable.

Data Sharing Statement: All data are available within the study.

Footnotes

Authorship Contributions:

Conceptualization: M.A.A.; Design/methodology: M.A.A.; Execution/investigation: B.R. and M.A.A.; Resources/materials: M.A.A.; Data acquisition: B.R. and M.A.A.; Data analysis/interpretation: B.R. and M.A.A.; Writing – original draft: B.R. and M.A.A.; Writing – review & editing/critical revision: M.A.A.

Conflict of Interest: The author(s) have no conflicts of interest to declare.

Funding: This study was supported by Ondokuz Mayıs University Scientific Research Projects Coordination Unit under project number BAP04-A-2024-4886.

References

Akkız, H., Şimşek, H., Balcı, D., Ülger, Y., Onan, E., Akçaer, N., & Delik, A. (2025). Inflammation and cancer: Molecular mechanisms and clinical consequences. *Frontiers in Oncology, 15*, 1564572. https://doi.org/10.3389/fonc.2025.1564572

Aranda-Anzaldo, A., Dent, M. A. R., Segura-Anaya, E., & Martinez-Gomez, A. (2024). Protein folding, cellular stress and cancer. *Progress in Biophysics and Molecular Biology, 191*, 40–57. https://doi.org/10.1016/j.pbiomolbio.2024.07.001

Balvan, J., Krizova, A., Gumulec, J., Raudenska, M., Sladek, Z., Sedlackova, M., Babula, P., Sztalmachova, M., Kizek, R., Chmelik, R., & Masarik, M. (2015). Multimodal holographic microscopy: Distinction between apoptosis and oncosis. *PLOS ONE, 10*(3), e0121674. https://doi.org/10.1371/journal.pone.0121674

Barrio, S., Gallardo, M., Arenas, A., Ayala, R., Rapado, I., Rueda, D., Jimenez-Ubieto, A., Albizua, E., Burgaleta, C., Gilsanz, F., & Martinez-Lopez, J. (2013). Inhibition of related JAK/STAT pathways with molecular targeted drugs shows strong synergy with ruxolitinib in chronic myeloproliferative neoplasm. *British Journal of Haematology, 161*(5), 667–676. https://doi.org/10.1111/bjh.12308

Bian, L., Yu, P., Wen, J., Li, N., Huang, W., Xie, X., & Ye, F. (2021). Survival benefit of platinum-based regimen in early stage triple negative breast cancer: A meta-analysis of randomized controlled trials. *NPJ Breast Cancer, 7*(1), 157. https://doi.org/10.1038/s41523-021-00367-w

Bou Zerdan, M., Ghorayeb, T., Saliba, F., Allam, S., Bou Zerdan, M., Yaghi, M., Bilani, N., Jaafar, R., & Nahleh, Z. (2022). Triple negative breast cancer: Updates on classification and treatment in 2021. *Cancers, 14*(5), 1253. https://doi.org/10.3390/cancers14051253

Brabec, V., & Kasparkova, J. (2005). Modifications of DNA by platinum complexes: Relation to resistance of tumors to platinum antitumor drugs. *Drug Resistance Updates, 8*(3), 131–146. https://doi.org/10.1016/j.drup.2005.04.006

Clowse, M. E., & Wigley, F. M. (2003). Digital necrosis related to carboplatin and gemcitabine therapy in systemic sclerosis. *The Journal of Rheumatology, 30*(6), 1341–1343. https://www.ncbi.nlm.nih.gov/pubmed/12784412

Dai, C., Whitesell, L., Rogers, A. B., & Lindquist, S. (2007). Heat shock factor 1 is a powerful multifaceted modifier of carcinogenesis. *Cell, 130*(6), 1005–1018. https://doi.org/10.1016/j.cell.2007.07.020

Desai, S., Liu, Z., Yao, J., Patel, N., Chen, J., Wu, Y., Ahn, E. E., Fodstad, O., & Tan, M. (2013). Heat shock factor 1 (HSF1) controls chemoresistance and autophagy through transcriptional regulation of autophagy-related protein 7 (ATG7). *Journal of Biological Chemistry, 288*(13), 9165–9176. https://doi.org/10.1074/jbc.M112.422071

Grunt, T. W., Somay, C., Pavelka, M., Ellinger, A., Dittrich, E., & Dittrich, C. (1991). The effects of dimethyl sulfoxide and retinoic acid on the cell growth and the phenotype of ovarian cancer cells. *Journal of Cell Science, 100*(3), 657–666. https://doi.org/10.1242/jcs.100.3.657

Hashmi, A. A., Ajaz, Y., Sajjad, M., Zia, F., Irfan, M., Abu Bakar, S. M., Khan, E. Y., & Faridi, N. (2025). Predictive value of excision repair cross complementation group 1 (ERCC1) by immunohistochemistry for determining neoadjuvant chemotherapy response in triple-negative breast cancers. *The Breast Journal, 2025*, 8410670. https://doi.org/10.1155/tbj/8410670

Hruban, R. H., Sternberg, S. S., Meyers, P., Fleisher, M., Menendez-Botet, C., & Boitnott, J. K. (1991). Fatal thrombocytopenia and liver failure associated with carboplatin therapy. *Cancer Investigation, 9*(3), 263–268. https://doi.org/10.3109/07357909109021323

Kawara, H., Akahori, R., Wakasugi, M., Sancar, A., & Matsunaga, T. (2019). DCAF7 is required for maintaining the cellular levels of ERCC1-XPF and nucleotide excision repair. *Biochemical and Biophysical Research Communications, 519*(1), 204–210. https://doi.org/10.1016/j.bbrc.2019.08.147

Kovács, D., Sigmond, T., Hotzi, B., Bohar, B., Fazekas, D., Deak, V., Vellai, T., & Barna, J. (2019). HSF1Base: A comprehensive database of HSF1 (heat shock factor 1) target genes. *International Journal of Molecular Sciences, 20*(22), 5815. https://doi.org/10.3390/ijms20225815

Lee, J. (2023). Current treatment landscape for early triple-negative breast cancer (TNBC). *Journal of Clinical Medicine, 12*(4), 1524. https://doi.org/10.3390/jcm12041524

Li, Q., Yu, J. J., Mu, C., Yunmbam, M. K., Slavsky, D., Cross, C. L., Bostick-Bruton, F., & Reed, E. (2000). Association between the level of ERCC-1 expression and the repair of cisplatin-induced DNA damage in human ovarian cancer cells. *Anticancer Research, 20*, 645–652.

Lin, C., Cui, J., Peng, Z., Qian, K., Wu, R., Cheng, Y., & Yin, W. (2022). Efficacy of platinum-based and non-platinum-based drugs on triple-negative breast cancer: Meta-analysis. *European Journal of Medical Research, 27*(1), 201. https://doi.org/10.1186/s40001-022-00839-0

Ma, E. L. B., & El Kashef, W. F. (2017). ERCC1 expression in metastatic triple negative breast cancer patients treated with platinum-based chemotherapy. *Asian Pacific Journal of Cancer Prevention, 18*(2), 507–513. https://doi.org/10.22034/APJCP.2017.18.2.507

Marteijn, J. A., Lans, H., Vermeulen, W., & Hoeijmakers, J. H. (2014). Understanding nucleotide excision repair and its roles in cancer and ageing. *Nature Reviews Molecular Cell Biology, 15*(7), 465–481. https://doi.org/10.1038/nrm3822

Mendillo, M. L., Santagata, S., Koeva, M., Bell, G. W., Hu, R., Tamimi, R. M., Fraenkel, E., Ince, T. A., Whitesell, L., & Lindquist, S. (2012). HSF1 drives a transcriptional program distinct from heat shock to support highly malignant human cancers. *Cell, 150*(3), 549–562. https://doi.org/10.1016/j.cell.2012.06.031

Metzger, R., Leichman, C. G., Danenberg, K. D., Danenberg, P. V., Lenz, H. J., Hayashi, K., Groshen, S., Salonga, D., Cohen, H., Laine, L., Crookes, P., Silberman, H., Baranda, J., Konda, B., & Leichman, L. (1998). ERCC1 mRNA levels complement thymidylate synthase mRNA levels in predicting response and survival for gastric cancer patients receiving combination cisplatin and fluorouracil chemotherapy. *Journal of Clinical Oncology, 16*(1), 309–316. https://doi.org/10.1200/JCO.1998.16.1.309

Page, T. J., Sikder, D., Yang, L., Pluta, L., Wolfinger, R. D., Kodadek, T., & Thomas, R. S. (2006). Genome-wide analysis of human HSF1 signaling reveals a transcriptional program linked to cellular adaptation and survival. *Molecular BioSystems, 2*(12), 627–639. https://doi.org/10.1039/b606129j

Pathak, N., Sharma, A., Elavarasi, A., Sankar, J., Deo, S. V. S., Sharma, D. N., Mathur, S., Kumar, S., Prasad, C. P., Kumar, A., & Batra, A. (2022). Moment of truth—Adding carboplatin to neoadjuvant/adjuvant chemotherapy in triple negative breast cancer improves overall survival: An individual participant data and trial-level meta-analysis. *The Breast, 64*, 7–18. https://doi.org/10.1016/j.breast.2022.04.006

Powers, M. V., & Workman, P. (2007). Inhibitors of the heat shock response: Biology and pharmacology. *FEBS Letters, 581*(19), 3758–3769. https://doi.org/10.1016/j.febslet.2007.05.040

Sidoni, A., Cartaginese, F., Colozza, M., Gori, S., & Crino, L. (2008). ERCC1 expression in triple negative breast carcinoma: The paradox revisited. *Breast Cancer Research and Treatment, 111*(3), 569–570. https://doi.org/10.1007/s10549-007-9804-4

de Sousa, G. F., Wlodarczyk, S. R., & Monteiro, G. (2014). Carboplatin: Molecular mechanisms of action associated with chemoresistance. *Brazilian Journal of Pharmaceutical Sciences, 50*(4), 693–701. https://doi.org/10.1590/S1984-82502014000400004

Tuncer, S., Gurbanov, R., Sheraj, I., Solel, E., Esenturk, O., & Banerjee, S. (2018). Low dose dimethyl sulfoxide driven gross molecular changes have the potential to interfere with various cellular processes. *Scientific Reports, 8*(1), 14828. https://doi.org/10.1038/s41598-018-33234-z

Verheijen, M., Lienhard, M., Schrooders, Y., Clayton, O., Nudischer, R., Boerno, S., Timmermann, B., Selevsek, N., Schlapbach, R., Gmuender, H., Gotta, S., Geraedts, J., Herwig, R., Kleinjans, J., & Caiment, F. (2019). DMSO induces drastic changes in human cellular processes and epigenetic landscape in vitro. *Scientific Reports, 9*(1), 4641. https://doi.org/10.1038/s41598-019-40660-0

Voorhees, P. M., Chen, Q., Kuhn, D. J., Small, G. W., Hunsucker, S. A., Strader, J. S., Corringham, R. E., Zaki, M. H., Nemeth, J. A., & Orlowski, R. Z. (2007). Inhibition of interleukin-6 signaling with CNTO 328 enhances the activity of bortezomib in preclinical models of multiple myeloma. *Clinical Cancer Research, 13*(21), 6469–6478. https://doi.org/10.1158/1078-0432.CCR-07-1293

Vyas, D., Laput, G., & Vyas, A. K. (2014). Chemotherapy-enhanced inflammation may lead to the failure of therapy and metastasis. *OncoTargets and Therapy, 7*, 1015–1023. https://doi.org/10.2147/OTT.S60114

Wang, S., Zhang, H., Cheng, L., Evans, C., & Pan, C. X. (2010). Analysis of the cytotoxic activity of carboplatin and gemcitabine combination. *Anticancer Research, 30*(11), 4573–4578. https://www.ncbi.nlm.nih.gov/pubmed/21115908

Welsh, C., Day, R., McGurk, C., Masters, J. R., Wood, R. D., & Koberle, B. (2004). Reduced levels of XPA, ERCC1 and XPF DNA repair proteins in testis tumor cell lines. *International Journal of Cancer, 110*(3), 352–361. https://doi.org/10.1002/ijc.20134

Yun, C. W., Kim, H. J., Lim, J. H., & Lee, S. H. (2019). Heat shock proteins: Agents of cancer development and therapeutic targets in anti-cancer therapy. *Cells, 9*(1), 60. https://doi.org/10.3390/cells9010060